2011 IEEE International Conference on Robotics and Automation
Shanghai International Conference Center
May 9-13, 2011, Shanghai, China

A High Dynamic Range Vision Approach to Outdoor Localization

Kiyoshi Irie, Tomoaki Yoshida, and Masahiro Tomono

***Abstract*— We propose a novel localization method for outdoor mobile robots using High Dynamic Range (HDR) vision technology. To obtain an HDR image, multiple images at different exposures is typically captured and combined. However, since mobile robots can be moving during a capture sequence, images cannot be fused easily. Instead, we generate a set of keypoints that incorporates those detected in each image. The position of the robot is estimated using the keypoint sets to match measured positions with a map. We conducted experimental comparisons of HDR and auto-exposure images, and our HDR method showed higher robustness and localization accuracy.**

I. Introduction

Outdoor navigation is an important aspect of mobile robotics, and localization is one of its crucial components. Although localization has been studied extensively and a number of methods have been proposed, robust and accurate localization in varying outdoor environments is still difficult.

We are pursuing vision-based methods for mobile robot localization. Recently, image features with distinctive local descriptors, such as Scale-invariant feature transform (SIFT), have been employed for localization [1] [2], which is effective for indoor environments. However, in outdoor environments, illumination conditions can change drastically, making it difficult to detect stable features.

Fig. 1 shows an example of SIFT keypoint detection in an outdoor environment. SIFT keypoints were detected in two images of the same place captured at different times. The two images appear very different because of the difference in the sun angle and the camera's limited dynamic range. We matched keypoints between the two images using Lowe's SIFT Keypoint Matcher [3]; only four keypoints of the 530 detected were correctly matched.

To cope with this illumination problem, High Dynamic Range (HDR) imagery has been employed [4]. One way to obtain an HDR image is exposure bracketing, which fuses multiple images captured at different exposures. We generated HDR images, detected SIFT keypoints, and matched them in the same way as for the auto-exposure images (Fig. 1, bottom) and found that the number of correct keypoint matches increased to 19. Thus, HDR imagery can improve the robustness of SIFT keypoint detection.

When HDR imagery is applied to mobile robots using exposure bracketing, images captured at different exposures may not be of the same scene, because the robot may be moving. This makes it difficult to fuse images to render an HDR image. To address this problem, we generate a set of keypoints merging those from multiple images at different exposures, instead of fusing images. We refer to this merged keypoint set as the *HDR Keypoint Set* in this paper.

All authors are with Future Robotics Technology Center, Chiba Institute of Technology, 2-17-1 Tsudanuma, Narashino-shi, Chiba , Japan {irie, yoshida, tomono}@furo.org

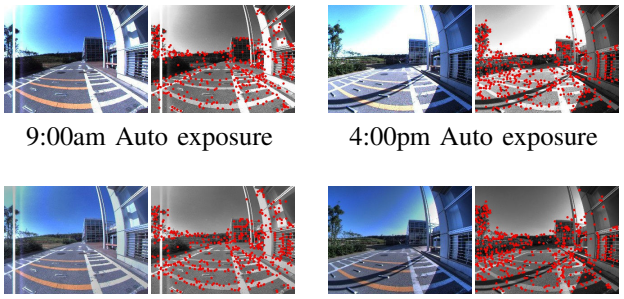

Fig. 1. Top: Two auto-exposure images of the same place captured at 9:00 am and 4:00 pm and their SIFT keypoint detection results. Red points indicate detected keypoints. Bottom: HDR images of the same place, rendered from four images captured at different exposures, and their SIFT keypoint detection results. Lowe's SIFT Keypoint Detector [3] was used to detect the SIFT keypoints. PhotomatixPro3.0 was used to render the HDR images.

We developed a new localization method using the HDR Keypoint Set. First, the robot is manually operated to collect images and generate a map of HDR Keypoint Sets. A particle filter is then employed to localize the robot during navigation. The particles are drawn according to odometry estimation and weighted by matching HDR Keypoint Sets between the map and a measurement based on an epipolar constraint.

The main contributions of this paper are twofold. The most significant one is a keypoint maintenance framework for HDR imagery that accommodates images captured at various times and camera poses. The other contribution is a particle filter based localization system that handles differences in time and camera pose between images.

We verified our method by localization experiments under different illumination conditions.

II. Related Work

A number of cameras that can acquire HDR images have been proposed. Some use HDR imaging devices [5] [6], and some are camera systems that capture multiple images and fuse them internally [4] [7]. These HDR cameras are usually expensive and are not widely available yet.

One method for producing an HDR image using conventional cameras (low dynamic range cameras) is to capture multiple images at different exposures and fuse them offline. It is widely used and many graphics editing software applications have this feature. Although it is a useful approach, it is not easily applicable to mobile robots, since it

requires the camera and the scene to be motionless during multiple captures.

Hrabar addressed this issue by fusing not images but occupancy information obtained from stereo vision [8]. However, this method assumes that all camera poses are known, and their paper does not discuss how to deal with problem of localization. In contrast, our method uses only relative camera poses between images, not absolute camera poses. Thus our method requires only locally reliable robot motion estimation (such as odometry), not the global position of the robot.

Outdoor localization methods using non-HDR vision have also been studied intensively, and methods such as the teaching-playback approach [9], occupancy map-matching using a stereo camera [10], and matching 3D points reconstructed by motion stereo [11] have been proposed.

Compared to these approaches, our method has an advantage in that the robot can navigate on paths that differ from the map. The computational cost of our method is relatively small because we use a monocular camera and do not use 3D reconstruction. Moreover, our method can use distant views or objects far from the camera, which can not be reconstructed by stereo vision approaches because of the small disparities in apparent position.

III. HDR KEYPOINT SET

In this section, we define the HDR Keypoint Set that we use instead of HDR images. The HDR Keypoint Set consists of a set of keypoints detected in a series of images and the relative camera poses between the images.

In the experiments described in this paper, we employed SIFT as a keypoint detector. However, the HDR Keypoint Set can also handle other image local features such as Speed Up Robust Features (SURF).

A. Definition of HDR Keypoint Set

Although it seems obvious that using multiple images captured at different exposures can improve the robustness to illumination conditions, adopting the approach for mobile robots requires that we relax the constraint that the camera must be still.

Our approach is to create a set of keypoints detected in source images. We use odometry to obtain the relative camera poses (relative position and rotation) between source images, assuming odometry is locally reliable. Keypoints are detected in each image and merged into a single set. Keypoints that appear in multiple images are extracted, grouped and handled as a single keypoint. This is done by matching keypoints between images and removing false matches by using the relative camera pose between images. We refer to this set of keypoints associated with relative camera poses as the *HDR Keypoint Set*.

Compared to a simple union of keypoint sets from multiple images, an HDR Keypoint Set has two advantages. First, the number of keypoints in a set is reduced, so the computational cost of matching keypoint sets can also be reduced. This is particularly effective when performing exhaustive matches of keypoint descriptors between keypoint sets. Second, keypoints that appear in multiple images at different exposures can be considered as robust to illumination conditions. The number of images that contain a keypoint can be used as a barometer of robustness or significance. Our localization method described below, uses it as a weight in keypoint matching.

B. Generation of HDR Keypoint Set

Assuming that n images are captured at different shutter speeds for an HDR Keypoint Set, we denote images by $I_1, I_2, ...I_n$ and the sets of keypoints detected in them as $K_1, K_2, ..., K_n$ in ascending order of shutter speed. Here we denote the union of keypoint sets detected in all images by

$$H' = K_1 \cup K_2 \cup ... \cup K_n. \tag{1}$$

Keypoints in $K_1, K_2, ..., K_n$ are matched between images to find keypoints that appear in multiple images. Those keypoints in H' are removed (excluding one of them) as "duplicated" and we obtain an HDR Keypoint Set:

$$H = H' - D \tag{2}$$

where D is a set of duplicated keypoints in H'. Finally, for each keypoint k in the HDR Keypoint Set, the number of images that contain the keypoint is registered as the importance of the keypoint.

C. Detecting Duplicated Keypoints

To find duplicated keypoints efficiently, only neighboring images are compared together. This is because if a keypoint in K_j is not found in K_{j+1} because of over exposure, it is not likely to appear in K_{j+2}. For each keypoint in $K_j (j = 0, ...n-1)$ is compared with all keypoints in K_{j+1} and find the closest keypoint by the Euclidean distance of their feature vectors. The matched keypoints are treated as a pair and stored in a set of matched pairs: M_j.

The set of matched pairs usually contains many false matches. Lowe removed false matches using the second-closest neighbor [12]; however, the method can also remove many correct matches. Our approach is to remove false matches using an epipolar constraint between images.

Essential matrix $\mathbf{E}$ is calculated using the relative rotation matrix R and normalized translation vector $t = [x, y, z]^T$ between two camera poses which is typically obtained from odometry.

$$t_\times = \begin{pmatrix} 0 & -z & y \\ z & 0 & -x \\ -y & x & 0 \end{pmatrix} \tag{3}$$

$$\mathbf{E} = t_\times R \tag{4}$$

We denote the 3D ray vector for a keypoint k by $\mathbf{p}_k$. Each matched keypoint pair (k_1, k_2) in M_j is evaluated as to whether it satisfies eq. (5); if not, it is removed from M_j.

$$|\mathbf{p}_{k_2}^T \mathbf{E} \mathbf{p}_{k_1}| < r_{th} \quad (r_{th} : \text{threshold}) \tag{5}$$

The procedure is applied to all $M_j (j = 0, ...n-1)$ to find all keypoints that appear in multiple source images.

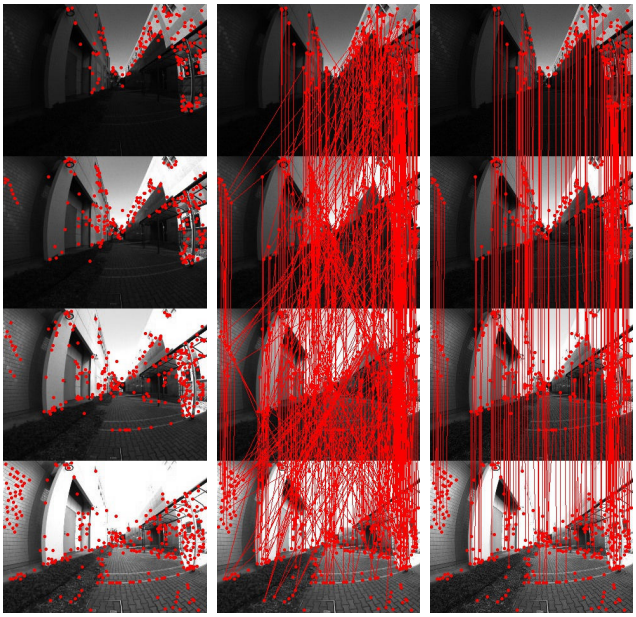

Fig. 2. Finding keypoints that appear in multiple images. Left: Keypoints detected by SIFT. Center: Matched pairs of keypoints. Right: False matches are removed by an epipolar constraint.

It should be noted that when two camera poses are the same (i.e. the camera is not moving), the epipolar constraint can not be calculated. In such a case, false matches can be easily found by comparing the position of the keypoints on the image coordinates.

Fig. 2 illustrates the process of finding keypoints that appear in multiple images.

IV. Localization using HDR Keypoint Set

Our localization method uses a single camera, and is based on Monte Carlo Localization [13]. The robot is assumed to navigate on a flat surface, and the 2D pose of the robot, $\mathbf{x} = (x, y, \theta)$, is estimated. A map consisting of a database of HDR Keypoint Sets is built in advance, and the pose of the robot is estimated on the map. To build a map, the robot is manually navigated along the path collecting images and odometry log. HDR Keypoint Sets are then generated and placed according to the odometry log.

A. Localization

In the prediction step, for each particle a new generation of particles $\mathbf{s}_t^{(i)}$ is drawn according to the probability of the robot's pose given the previous state $\mathbf{s}_{t-1}^{(i)}$ and the relative movement of the robot $\Delta\mathbf{x}_t$.

$$\mathbf{s}_t^{(i)} \sim p(\mathbf{x}_t|\mathbf{s}_{t-1}^{(i)}, \Delta\mathbf{x}_t) \tag{6}$$

In our implementation, we use odometry to obtain the relative motion of the robot and assume errors in the odometry follow a normal distribution.

Subsequently, a series of images are captured at different exposures, and a measurement HDR Keypoint Set H_t is generated. The particles are updated by weighting each particle using the likelihood of H_t given map M and the particles $\mathbf{s}_t^{(i)}$ as shown in eq. (7).

$$p(H_t|\mathbf{s}_t^{(i)}, \mathbf{M}) \tag{7}$$

Since the true distribution of eq. (7) is difficult to determine, we would like to obtain a distribution similar to it. Our method approximates it using the number of correct keypoint matches between the measurement and the map.

For each particle i, the HDR Keypoint Set entry H_{map}^i that is closest to the pose of the particle is chosen from the map (see section IV-B for details). Keypoints in H_t and H_{map}^i are matched to create a set of matched pairs:

$$M_{t,map}^i = \{(k_1, k_2)|k_1 \in H_t, k_2 \in H_{map}^i\} \tag{8}$$

The particles are scored by counting the number of matched pairs that satisfy the epipolar constraint. The epipolar constraint is evaluated for each matched pair $(k_1, k_2) \in M_{t,map}^i$ using ray vectors of the keypoints $\mathbf{p}_{k_1}, \mathbf{p}_{k_2}$ and the essential matrix $\mathbf{E}_{k_1,k_2}$. The essential matrix for the relative camera pose between the measurement and the map is calculated as eq. (4). The relative camera pose is calculated using the robot pose of H_{map}^i on the map and the pose of the particle at the time the image was captured.

We have found that incorporating the importance of the keypoint (see section III-B) improves the accuracy of localization. We denote the importance of keypoint k by m_k. The score of a particle is calculated as the sum of the weighted number of matched pairs that satisfy the epipolar constraint (eq. (9)-(11)).

$$r_{k_1,k_2} = |\mathbf{p}_{k_2}^T \mathbf{E}_{k_1,k_2} \mathbf{p}_{k_1}| \tag{9}$$

$$f_s(k_1, k_2) = \begin{cases} m_{k1} \cdot m_{k_2} & (\text{if} \quad r_{k_1,k_2} < r_{th}) \\ 0 & (\text{otherwise}) \end{cases} \tag{10}$$

$$W^{(i)} = \frac{\sum_{[k_1,k_2] \in M_{t,map}^i} f_s(k_1, k_2)}{\sum_{k_2 \in H_{map}^i} m_{k_2}} \tag{11}$$

Finally, particles are resampled using a normalized weight:

$$w^{(i)} = W^{(i)} / \sum_j W^{(j)}. \tag{12}$$

B. Choosing Matching Candidates from Map

A caveat in evaluating a keypoint pair using the epipolar constraint is that the translation between the camera poses of the measurement and the map must not be zero. Because if the translation is zero, eq. (9) is always zero even for any false matches. We avoid this problem by choosing an HDR Keypoint Set entry from the map that is closest to the pose of the particle but not closer than a threshold.

Matching keypoints between HDR Keypoint Sets is the most time-consuming task in weighting and resampling particles. In particular, when the distribution of the particles is large (e.g., the robot's pose is completely unknown), the number of comparisons is also large because many particles choose different map entries. We could reduce the computational cost by updating particles on the basis of

Fig. 3. Robot used in experiments.

measurements using image searching (e.g., FAB-MAP [14] and Vocabulary Tree [15]).

V. Experiments

A. System Description

Our robot PapyrusII (Fig. 3) has a gyro-assisted odometry system [16]. A camera HMB-2000 from VSharp Inc., consisting of a Grasshopper (Point Grey Research Inc.) and a fish-eye lens, is mounted at a height of $80cm$. The camera has a field of view of 185° in both vertical and horizontal directions, and is capable of capturing images at 15fps, cycling four user-defined exposure settings (gain and shutter speed) [17].

Since the camera does not have any automatic shutter speed and gain control for HDR images, we implemented a simple shutter speed control system for HDR images; the fastest shutter speed t_1[ms] is chosen using the average pixel intensity of the previous image and the rest three shutter speeds are determined as $t_2 = 2t_1, t_3 = 4t_1, t_4 = 8t_1$. Images were shrunk to 512×512 in the experiments.

B. All-day Keypoint Matching

The robustness of keypoint matching was evaluated. Both HDR and auto-exposure images of the same scene were captured from 10:00am to 3:00pm on a sunny day. Images captured at 1:00pm were matched with images captured at different time of day. The result shown in Fig. 4 indicates that the number and the ratio of correct keypoint matches are improved by the HDR Keypoint Set.

C. Position Tracking In a Small Loop

We conducted position tracking experiments on a loop of $400m$ in our campus that includes paved roads and tiled pedestrian areas. To evaluate the effectiveness of introducing the HDR method, we collected both HDR images and auto-exposure images simultaneously and split them into two data sets (HDR and auto-exposure) that share the same odometry log. In collecting the data sets, the robot was manually navigated along the path at a maximum speed of $60cm/s$, capturing five images (one auto-exposure image and four images at different exposures) at every 3 seconds. The robot was operated to pass through 16 reference points in the path that we have defined to measure the localization accuracy.

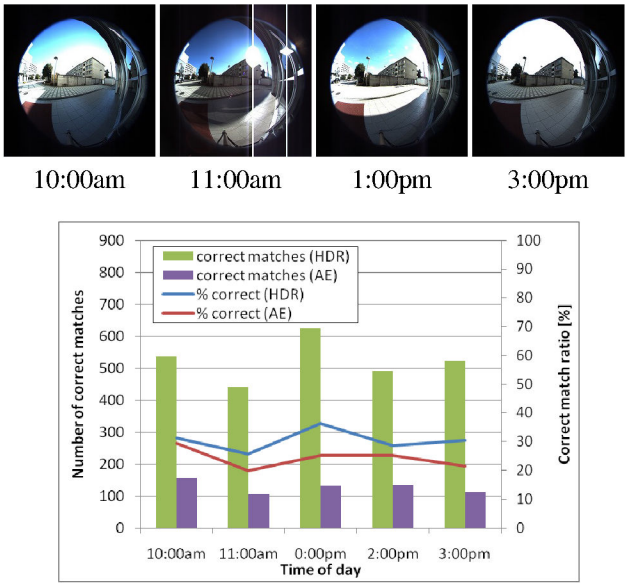

Fig. 4. Keypoint matching experiments. Top: Images from keypoint matching experiments. Bottom: Matching results.

We collected three data sets at 9:00 am, 3:30 pm, and 4:00 pm on three shiny days. Images collected by the robot are shown in Fig. 5. In experiments below, the initial pose of the robot is given as a normal distribution with a standard deviation of $50cm$ and the number of particles employed was 300.

1) Accuracy: We measured the accuracy of our localization method using the three data sets. Each data set in turn is used as a map and an input to localization. Loops in the odometry log were closed by the Lu-Milios method [18] in constructing the maps. In addition to the comparison between our HDR method and auto-exposure method, we investigated how merging keypoints in constructing a HDR Keypoint Set affects the localization accuracy. Table. I summarizes the results. The proposed method showed higher accuracy when the illumination conditions between the map and the input differ largely (Table. I a, c); no significant difference is found when the illumination conditions in the map and the input are similar (b). Our method with the HDR Keypoint Set outperformed the simple union of keypoint set. The result can be interpreted that the HDR Keypoint Set detected keypoints that are robust to illumination conditions.

The trajectory of the estimated pose obtained in experiment (a) is shown in Fig. 6.

2) Performance: As described in section III, the HDR Keypoint Set groups and merges keypoints that appear multiple images and handles them as a single keypoint. We examined how the performance is influenced by merging keypoints. We used the data sets same as Table. I (a) and measured the computational time of particle updating procedure (excluding SIFT keypoint detection, including generation of a measurement HDR Keypoint Set) with two methods: our method using the proposed HDR Keypoint Set, and a method that uses a union of keypoint sets.

The comparison of the computational time along with the

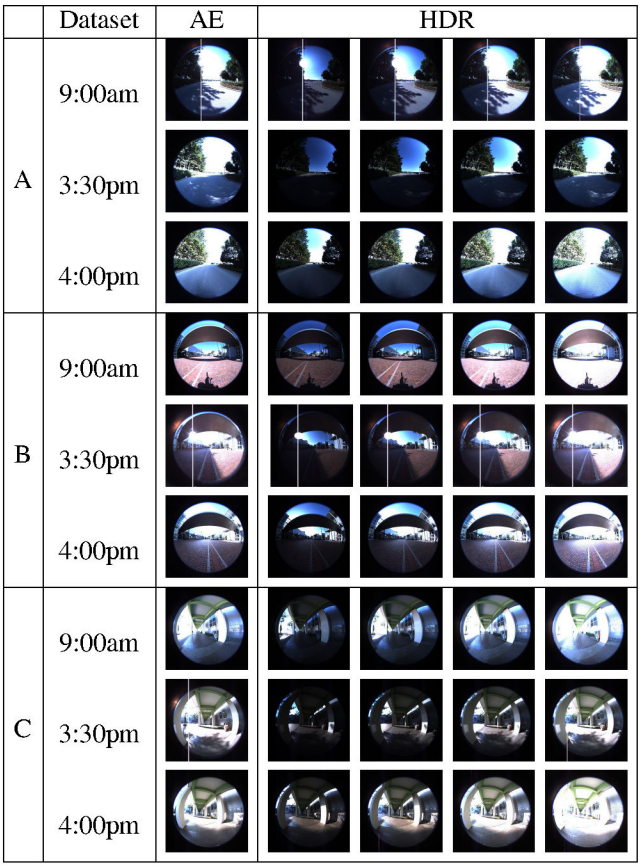

Fig. 5. Images captured by the robot at three points.

TABLE I

RESULT OF POSITION TRACKING EXPERIMENTS

	Input	Map	Method	Ave. Error	Max. Error
a	9:00am	3:30pm	HDR1*	24cm, 1.3°	61cm, 4.3°
			HDR2†	31cm, 1.3°	64cm, 4.2°
			AE‡	77cm, 2.0°	194cm, 5.6°
b	3:30pm	4:00pm	HDR1	12cm, 1.6°	25cm, 3.0°
			HDR2	12cm, 1.6°	34cm, 3.0°
			AE	12cm, 1.8°	29cm, 3.2°
c	4:00pm	9:00am	HDR1	50cm, 2.0°	185cm, 4.7°
			HDR2	203cm, 1.9°	415cm, 4.5°
			AE	512cm, 5.2°	993cm, 9.7°

* HDR Keypoint Set (proposed method)
† Union of HDR keypoints
‡ Auto-exposure

number of keypoints is shown in Fig. 7. The average updating time was 812ms by our method and 1,285ms by the method that uses a union of keypoint sets. Significant reductions of the computational time have been seen particularly when the number of keypoints was large. Keypoints were rather evenly detected in images with different shutter speeds.

3) Robustness: Two tests to evaluate the robustness on the proposed method were performed; one is using distorted odometry logs and the other is using partially occluded measurements. We generated distorted odometry logs based on the data set of 9:00 am; on each step in the odometry log, a Gaussian random error was added in both the position and the orientation of the robot. We used Gaussian errors with different standard deviations: 1, 3, 5, and 10% of the distance traveled; 0.1, 0.3, 0.5, and 1.0 deg/sec for the time elapsed. Occluded measurements are simulated by masking part of input images. We used masks with the size of 5, 10, 20, and 30% of the image.

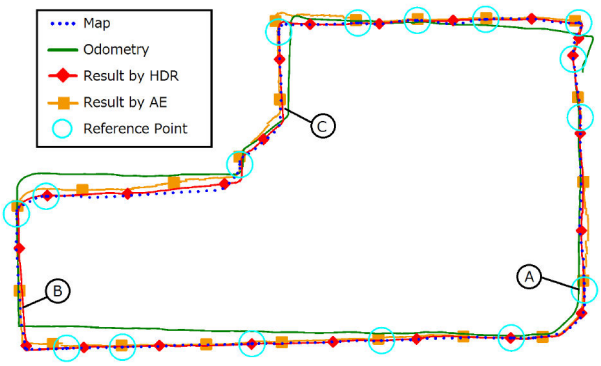

Fig. 6. Position tracking result by our proposed method (red) and auto-exposure method (orange). A, B, C indicates the points where images in Fig. 5 were captured.

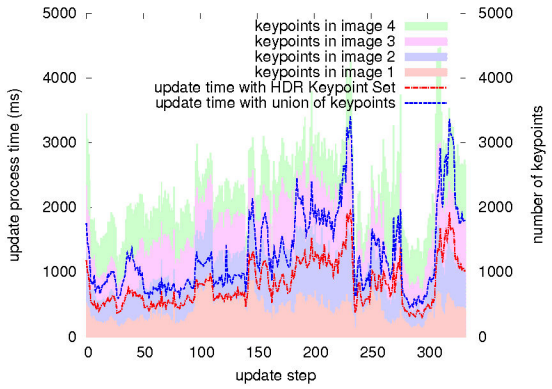

Fig. 7. Comparison of computational time for updating particles. Bars indicate the number of keypoints detected from each image. Image 1 is the one captured with the fastest shutter speed. The computational time was measured on a laptop with Core i7 3.33GHz.

Fig. 8 shows the accuracy of the position tracking experiments. Our method kept good localization accuracy with distorted odometry up to 5% error in distance and 0.5 deg/sec in orientation, and with 20% occluded input images.

D. Localization in a Larger Environment

Lastly, we tested our method in a larger environment. We generated a campus map using two data sets collected at 9:00 am and 9:30 am on different days. The distance that the robot traveled was 1.2km in total. The Lu-Milios method [18] was again used to arrange two data sets.

We then collected another data set at 4:20 pm by manually navigating the robot on a path that differs from the two paths used for the map, and conducted a position tracking experiment using the data set and the map. Our method successfully kept track of the robot's pose as shown in Fig. 9. We measured the accuracy at 21 reference points in the path; the average error was 83cm, 2.2° and the maximum error was 164cm, 10.2°.

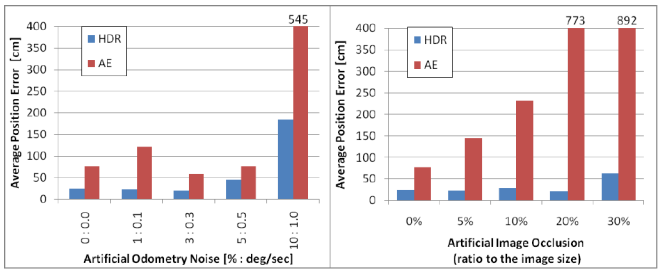

Fig. 8. The accuracy of localization using distorted odometry logs (left) and using partially occluded images (right).

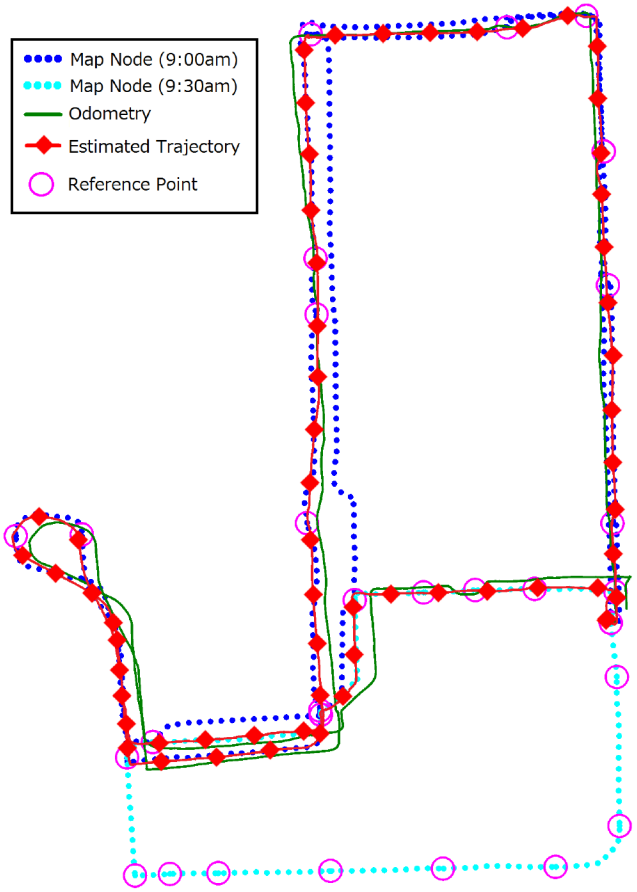

Fig. 9. Localization experiment in a larger environment. The estimated robot's trajectory by our method is shown in red. The map nodes generated from 9:00 am data set and 9:30 am data set are shown in blue and cyan dots, respectively.

VI. Conclusion

In this paper, we presented a localization method using a High Dynamic Range vision to cope with outdoor illumination issues. Instead of fusing images captured at different exposures, our method creates a set of keypoints incorporating keypoints detected in each image. The principal benefit of introducing High Dynamic Range vision is the increased number of keypoints. We have demonstrated that our HDR Keypoint Set approach improves keypoint-based localization in terms of the robustness, the accuracy and the computational cost.

Remaining topics include how to determine the optimal number of images and the exposures for a HDR Keypoint Set. An image histogram should be a help, and the number of keypoints and the distribution of keypoints in an image could also be used. We are also working on global localization using visual words approach.

While we consider the High Dynamic Range requisite for outdoor vision, we do not expect it to solve all of the illumination issues. For example, HDR might not be a solution to a problem that keypoints caused by sharp edges of shadows can affect keypoint matches. Some other technologies such as shadow removal should be required.

References

[1] S. Se, D. Lowe, and J. Little, "Local and global localization for mobile robots using visual landmarks," in *Proc. of the IEEE Int. Conf. on Intelligent Robots & Systems (IROS)*, vol. 1, 2001, pp. 414–420.

[2] J. Wang, R. Cipolla, and H. Zha, "Vision-based global localization using a visual vocabulary," in *Proc. of the IEEE Int. Conf. on Robotics & Automation (ICRA)*, 2005, pp. 4230–4235.

[3] D. Lowe. (2005) Demo software: SIFT keypoint detector. [Online]. Available: http://www.cs.ubc.ca/~lowe/keypoints/

[4] K. Yamada, T. Nakano, and S. Yamamoto, "A vision sensor having an expanded dynamic range for autonomous vehicles," *IEEE Transactions on Vehicular Technology*, vol. 47, no. 1, pp. 332–341, 1998.

[5] D. Stoppa, A. Simoni, L. Gonzo, M. Gottardi, and G.-F. D. Betta, "138dB dynamic range CMOS image sensor with new pixel architecture," in *Digests of the IEEE International Solid State Circuits Conference,*, 2002, pp. 40–41.

[6] M. Schanz, C. Nitta, A. Bussmann, B. Hosticka, and R. Wertheimer, "A high-dynamic-range CMOS image sensor for automotive applications," *IEEE Journal of Solid-State Circuits,*, vol. 35, no. 7, pp. 932–938, 2000.

[7] P. Burt and R. Kolczynski, "Enhanced image capture through fusion," in *Proc. of Fourth Int. Conf. on Computer Vision,*, 1993, pp. 173–182.

[8] S. Hrabar, P. Corke, and M. Bosse, "High dynamic range stereo vision for outdoor mobile robotics," in *Proc. of the IEEE Int. Conf. on Robotics & Automation (ICRA)*, 2009, pp. 430–435.

[9] Y. Yamagi, J. Ido, K. Takemura, Y. Matsumoto, J. Takamatsu, and T. Ogasawara, "View-sequece based indoor/outdoor navigation robust to illumination changes," in *Proc. of the IEEE Int. Conf. on Intelligent Robots & Systems (IROS)*, 2009, pp. 1229–1234.

[10] K. Irie, T. Yoshida, and M. Tomono, "Mobile robot localization using stereo vision in outdoor environments under various illumination conditions," in *Proc. of the IEEE Int. Conf. on Intelligent Robots & Systems (IROS)*, 2010, pp. 5175–5181.

[11] E. Royer, M. Lhuillier, M. Dhome, and J.-M. Lavest, "Monocular vision for mobile robot localization and autonomous navigation," *Int. J. of Computer Vision*, vol. 74, no. 3, pp. 237–260, 2007.

[12] D. G. Lowe, "Distinctive image features from scale-invariant keypoints," *Int. J. of Computer Vision*, vol. 60, no. 2, pp. 91–110, 2004.

[13] F. Dellaert, D. Fox, W. Burgard, and S. Thrun, "Monte carlo localization for mobile robots," in *Proc. of the IEEE Int. Conf. on Robotics & Automation (ICRA)*, 1999, pp. 1322–1328.

[14] M. Cummins and P. Newman, "FAB-MAP: Probabilistic localization and mapping in the space of appearance," *The Int. J. of Robotics Research*, vol. 6, no. 27, pp. 647–665, 2008.

[15] D. Nister and H. Stewenius, "Scalable recognition with a vocabulary tree," in *Proc. of the 2006 IEEE Computer Society Conference on Computer Vision and Pattern Recognition*, 2006, pp. 2161–2168.

[16] T. Yoshida, K. Irie, E. Koyanagi, and M. Tomono, "A sensor platform for outdoor navigation using gyro-assisted odometry and roundly-swinging 3D laser scanner," in *Proc. of the IEEE Int. Conf. on Intelligent Robots & Systems (IROS)*, 2010, pp. 1414–1420.

[17] Point Grey Research. (2010) Grasshopper technical reference manual. [Online]. Available: http://www.ptgrey.com/products/grasshopper/

[18] F. Lu and E. Milios, "Globally consistent range scan alignment for environment mapping," *Autonomous Robots*, vol. 4, pp. 333–349, 1997.